E-ISSN: 2709-9423
P-ISSN: 2709-9415
JRC 2023; 4(2): 111-117

www.chemistryjournal.net
Received: 06-05-2023
Accepted: 19-06-2023

Shiva Arun
Department of Chemistry, Dr. Shakuntala Misra National Rehabilitation University, Lucknow, Uttar Pradesh, India

Roop Kumar
Department of Chemistry, Dr. Shakuntala Misra National Rehabilitation University, Lucknow, Uttar Pradesh, India

Susheel Kumar Singh
Department of Physics, Dr. Shakuntala Misra National Rehabilitation University, Lucknow, Uttar Pradesh, India

Amit Kumar Tripathi
1. Department of Chemistry, Dr. Shakuntala Misra National Rehabilitation University, Lucknow, Uttar Pradesh, India
2. Department of Chemistry, Dr. Shakuntala Misra National Rehabilitation University, Lucknow, Uttar Pradesh, India

Krishna Srivastava
Department of Chemistry, Shri Ramswaroop Memorial University, Lucknow, Uttar Pradesh, India

Puspendra Singh
Department of Chemistry, Dr. Shakuntala Misra National Rehabilitation University, Lucknow, Uttar Pradesh, India

Correspondence
Puspendra Singh
Department of Chemistry, Dr. Shakuntala Misra National Rehabilitation University, Lucknow, Uttar Pradesh, India

Polyoxometalate based nanohybrid: Study of its antimicrobial activity

Shiva Arun, Roop Kumar, Susheel Kumar Singh, Amit Kumar Tripathi, Krishna Srivastava and Puspendra Singh

Abstract
The study of nanohybrids made by encasing polyoxometalates (POMs) in chitosan and their potential uses in medicine is a rapidly developing topic. This study involved the synthesis of a polyoxometalate ($K_8SiW_{11}O_{39}$) possessing a lacunary position in its Keggin type structure. Followed by insertion of alkylsilane into the lacunary location. It was subsequently subjected to a reaction with 2-hydroxy-1-naphtaldehyde, Ferric metalation, and then encapsulation into chitosan via the ionotropic gelation process, wherein the POM and the chitosan functioned as an anion and cation, respectively. The bands present in the UV-Vis spectra at distinct wavelengths signify the successful insertion of the alkylsilane into $K_8SiW_{11}O_{39}$, followed by Fe metalization. In order to create the final nanohybrid, its encapsulation into chitosan has been verified by UV-Vis spectroscopy. Moreover, FT-IR analysis was used to characterize chitosan, POM injected with alkylsilane, and nanohybrid. The complete set of anticipated elements is present in the nanohybrid, according to EDX analysis. Bacterial strains of B. subtilis gram (+)ve and E. Coli gram (-)ve were used to assess the antibacterial activity of POM implanted with alkylsilane and Nanohybrid. Comparing the nanohybrid to bare POM injected with metallated alkylsilane and chitosan has improved the hybrid's antibacterial activity.

Keywords: Nanohybrid, polyoxometalate, alkylsilane, antimicrobial activity

1. Introduction
Chitosan (CS) is a biocompatible polymer which has noteworthy uses in the field of biomedical science. CS is a polysaccharide that is derived in the chitin form from the exoskeleton of shrimp and the shells of crustaceans. With its high degree of biocompatibility, antibacterial, antifungal, and wound-healing qualities, CS is found in large quantities in nature [1, 2]. Biocompatible CS has been thoroughly investigated in the human body for the transportation of different medications, vaccinations, and genes [3].
High oxidation states of polyoxometalates (POMs) form stable oxoclusters with transition metal (usually W, V, Mo and W) that vary in size and composition. Because of these properties, POMs have gained interest for a wide range of applications in biomedicine, catalysis, luminescence, magnetics, dye degradation, and other areas [4]. Because POM-based systems have shown to be a valuable tool for use in antibacterial, antiviral, and anticancer actions, research on them has risen [5]. POM's lacunary position can be used to create a variety of hybrids with a range of useful qualities and uses [6].
POMs with bioactivity that are encapsulated in biodegradable CS polymer present a number of opportunities for the creation of pharmaceuticals [7, 8] with improved stability at varying pH values [9], high potential bioactivity with low toxicity, and efficient bio distribution [10]. First, a stable lacunary POM molecule ($K_8[SiW_{11}O_{39}].13H_2O$) (LPOM) was created in the current research report by releasing one tungstate unit from its saturated parent chemical ($K_8[SiW_{12}O_{40}]. xH_2O$) [11]. The "cavity" known as the "lacunary hole" in the LPOM molecule has been inserted with the alkylsilane 3-(Triethoxysilyl)propylamine (LPOM-Sil). It was then combined with 2-hydroxy-1-naphtaldehyde to create LPOM-Sil-HN, which was further metalated with Fe to create LPOM-Sil-HN-Fe. To improve the antibacterial property, LPOM-Sil-HN has undergone Fe metalation. LPOM-Sil-HN-Fe has been finally encapsulated into CS to form a NHybd. Testing has been done on CS, LPOM-Sil-HN-Fe, and NHybd against gram (+) ve and gram(-)ve strains of B. subtilis and E. coli, respectively.

2. Experimental Section

2.1 Materials and Characterization Techniques

CS (low molecular weight), silicotungstic acid $H_4[SiW_{12}O_{40}]xH_2O$, Ferric chloride anhydrous, tetrahexylammonium bromide, 3-(Triethoxysilyl) propylamine, 2-hydroxy-1-naphthaldehyde, and trimethylorthoformate (A.R. grade) were purchased from CDH and used without further purification. Potassium bicarbonate, acetic acid, ethanol have been purchased from CDH and are of A.R. grade. Nutrient broth and Nutrient agar have been purchased from Titan Biotech Ltd. Rajasthan, India. The test strain B. Subtilis gram(+)ve. bacteria and E.Coli gram (-)ve bacteria have been obtained from IMTECH, Chandigarh, India. FT-IR spectra have been recorded in the range of wave number 4000–300 cm-1 using KBr disks with Perkin Elmer spectrophotometer. For detecting the elemental composition of hybrid EDX detector has been used. Shimadzu UV-2450 has been used to record UV–visible spectra.

2.2.1 Preparation of LPOM

Tézé and Hervé[11] method has been followed for development of LPOM. FT-IR(cm^{-1}, KBr): 536, 710, 742, 797, 852, 870, 909, 950. By first functionalizing the alkylsilane {3-(Triethoxysilyl)propylamine $(C_2H_5\text{-}O)_3\text{-}Si\text{-}(CH_2)_3\text{-}NH_2\bullet HCl\}$, as per Bar-Nahum *et al.* [12], and then incorporating it in the lacunary site of LPOM (Scheme1), thus synthesizing $\{SiW_{11}O_{39}[O(Si\text{-}CH_2\text{-}CH_2\text{-}CH_2\text{-}NH_2\bullet HCl)_2]\}^{4-}$. To obtain the tetrahexylammonium $(n\text{-}hexyl)_4N^+)$ salt of LPOM-Sil, or $Q_4\{SiW_{11}O_{39}[O(Si\text{-}CH_2\text{-}CH_2\text{-}CH_2\text{-}NH2\bullet HCl)2]\}$, where Q = $(n\text{-}hexyl)_4N^+)$, tetrahexylammonium bromide has been added. 540, 720, 760, 794, 852, 870, 910, 954, 1045, 1158, 1230, 1480, 2948, 3245, 3446 are the FT-IR (cm^{-1}, KBr) values.

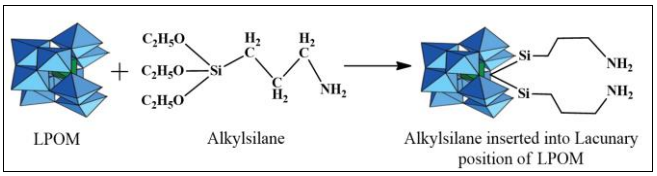

Scheme 1: Schematic presentation for synthesis of LPOM-Sil by insertion of Alkylsilane into LPOM

In addition, $Q_4\{SiW_{11}O_{39}\text{-}[O\text{-}(Si\text{-}CH_2\text{-}CH_2\text{-}CH_2\text{-}NH_2\text{*}HCl)_2]\}$ has been modified by attaching 2-hydroxy-1-naphthaldehyde to it in order to create $Q_4\{SiW_{11}O_{39}[O\text{-}(Si\text{-}CH_2\text{-}CH_2\text{-}CH_2\text{-}N{=}CH(2\text{-}OH\text{-}Naph)_2]\}$ (LPOM-Sil-HN) [13]. After dissolving 0.735 gm (0.42 mmol) of 2-hydroxy-1-naphthaldehyde in absolute methanol, 0.9 gm (0.21 mmol) of LPOM-Sil salt was added, and the mixture was constantly stirred for 24 hours at 25˚C (±1˚C) (Scheme2). Trimethylorthoformate (8 ml) was added to this mixture as a drying agent, and it was stirred at 25˚C (±1˚C) for the whole night.

After filtering and repeatedly washing with dry ether, a light brownish precipitate was produced. 534, 710, 741, 795, 850, 872, 910, 953, 1045, 1156, 1230, 1481, 1614, 1632, 2946, 3241, 3446 are the FT-IR (cm^{-1}, KBr) results.

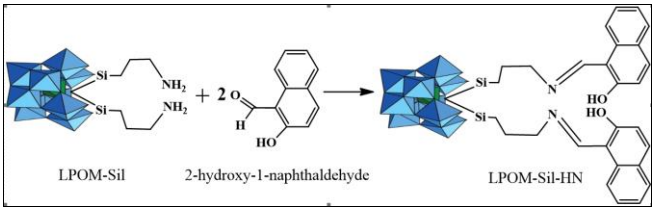

Scheme 2: Schematic presentation of 2-hydroxy-1-naphthaldehyde attached to LPOM-Sil

The same metalation process as described in Bar-Nahum *et al.* [12] article was used to create LPOM-Sil-HN-Fe (Scheme3). 1.5 g (0.32 mmol) of LPOM-Sil-HN was dissolved in 5 mL of degassed DMF and heated to 70 ˚C in an inert Argon environment while being constantly stirred, as per Scheme 3. To the aforementioned solution, 0.32 mmol of anhydrous copper acetate in DMF was added. The mixture was then kept at 75˚C (±1˚C) for 50 minutes before being cooled to 27˚C (±1˚C). After adding 35 mL of methanol, the precipitate was filtered, carefully cleaned with ether and methanol, and vacuum-dried. For LPOM-Sil-HN-Fe (Chemical formula: $C_{28}H_{30}FeN_2O_{42}Si_3W_{11}$; molecular weight: 3229.35; color: brownish red), the elemental analysis performed by CHNO yielded the following results: % C, 10.42; H, 0.94; N, 0.87; O, 20.81; found % C, 10.44; H, 0.96; N, 0.87; O, 20.84.

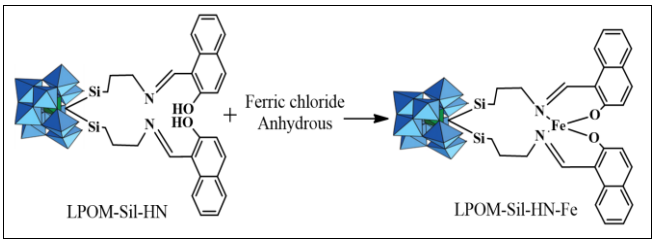

Scheme 3: Schematic presentation of Metalation of LPOM-Sil-HN with Ferric Chloride Anhydrous to synthesize LPOM-Sil-HN-Fe

NHybd has been prepared using the ionotropic gelation technique by previously reported method, in which the chitosan and the POM served as cation and anion, respectively[5(c)]. In order to synthesize NHybd comprising of CS and LPOM-Sil-HN-Fe (Scheme 4), CS has been dissolved in 2% v/v acetic acid to give concentrations of 0.50% w/v. The CS solution filtered to remove any suspended particles and heated at 50 ˚C for 2 hours with continuous stirring and then cooled to room temperature (Solution1). pH of above solution (Solution1) has been maintained at 6.5 with NaOH. 0.1 gm of LPOM-Sil-HN-Fe dissolved in minimum amount of milli-Q water (Solution2). Solution2 has been added to Solution1 drop-wise under the controlled sonication for 10 minutes resulting into a stable colloidal suspension of LPOM-Sil-HN-Fe and CS nano-hybrid which is hereafter abbreviated as NHybd. This colloidal suspension containing NHybd has been stirred at room temperature for 10 hours (h) and then centrifuged for 20 minutes (min), at 20,000rpm to collect NHybd. The NHybd of CS and LPOM-Sil-HN-Fe was collected and washed with milli-Q water several times and dried under vacuum.

LPOM-Silane-1H1N-Fe + Chitosan ⟶ NHybd

Scheme 4: Schematic presentation for synthesis of NHyd by encapsulation of LPOM-Sil-HN-Fe into CS

2. Study on Antibacterial Activity

Two bacterial strains, B. subtilis gram (+) ve and E. coli gram (-) ve, has been used in the antibacterial investigation of prepared NHybd and bare LPOM-Sil-NH-Fe. The agar diffusion method, has been used to conduct the antibacterial test. The fresh overnight culture in sterilized Nutrient Broth (13 g/L) was used to create the bacterial strain inoculum, which was then incubated at 37 °C. Nutrient agar that has been sterilized was poured into petri dishes and allowed to dry in order to implement the diffusion technique. Then, each bacterial strain's active broth culture (1% of the bacterial culture is needed to produce 105 CFU mL-1). Agar plates that had been inoculated were placed in 8 mm wells containing water as the control and were treated with bare LPOM-Sil-NH-Fe and NHybd in 100µl of aqueous solution. To ascertain the antibacterial efficacy, the incubation was carried out at 37 °C for an additional night. Afterwards, the diameter of the zone of inhibition was measured in millimeters.

3. Results and Discussions

3.1 FT-IR spectra

Appearance of similar FT-IR(cm^{-1}) bands (fig. 1a) as reported in reference[12]confirmed the formation of (α-$K_8SiW_{11}O_{39}$). Successful incorporation of alkylsilane$Q_4\{SiW_{11}O_{39}$-$[O(Si\text{-}CH_2\text{-}CH_2\text{-}CH_2\text{-}NH_2{*}HCl)_2]\}$ into the lacunary position of (α-$K_8SiW_{11}O_{39}$) for the formation of LPOM-Silanehas been confirmed by the occurrence of FT-IR bands (fig. 1b)at 1045 (υ_{asym} Si-O-Si), 1155 (C-N), 1232(Si-C), 1482 (C-H), 2948 (C-H), 3240 (N-H), 3445 (N-H) along with LPOM peaks at 535 (υ_{sym} WOW), 710 (υ_{asym} WOW), 741 (υ_{asym} WOW), 797 (υ_{asym} WOW), 852 (υ_{asym} WOW), 870 (υ_{asym} WOW), 909 (υ_{asym} W=O), 955 (υ_{asym} W=O). Similar FT-IR behavior has been reported by earlier workers [6]. The formation of LPOM-Sil-NH has been confirmed by the covalent attachment of 2-hydroxy-1-naphthaldehyde to the N atom of alkylsilane through the C atom of carbonyl group. This has been confirmed by the emergence of two new peaks of (C=N) at 1614 and 1632, in addition to the previously mentioned IR peaks with minute shifts (fig. 1c). The persistence of the Keggin structure of LPOM was confirmed in Figure 1c by the presence of unaffected FT-IR bands, even after LPOM-Sil was modified by covalently attaching 2-hydroxy-1-naphthaldehyde. The FT-IR spectrum of LPOM-Sil-NH-Fe, which has been recorded up to the far infra-red region, or 300, for the metalation of LPOM-Sil-HN, is displayed in Figure 1(a). The stretching vibration of the Fe-N bond, which indicates that Fe has been coordinated through N of C=N, is responsible for the FT-IR band at 445. The stretching vibration of the Fe-O bond, which is the deprotonated –O-H- group of 2-hydroxy-1-naphthaldehyde, is responsible for the band at 605 [16]. The FT-IR bands of CS are displayed in Figure 2(b), where the peak at 1636, which is characteristic, corresponds to N-H bending vibration (amines), and the peak at 1072, which is caused by bridge oxygen (C-O-C) stretching vibration [14]. The broad peak~ 3400 in the FT-IR spectrum of NH (Fig. 2c) corresponds to the –OH group, while the peak at 1636 is caused by the $–NH_2$ N-H bend. Additionally, NHybd exhibits the same distinctive FT-IR peaks that are seen in CS and LPOM-Sil-NH-Fe, with a minor shift which indicates the encapsulation of LPOM-Sil-NH-Fe into CS.

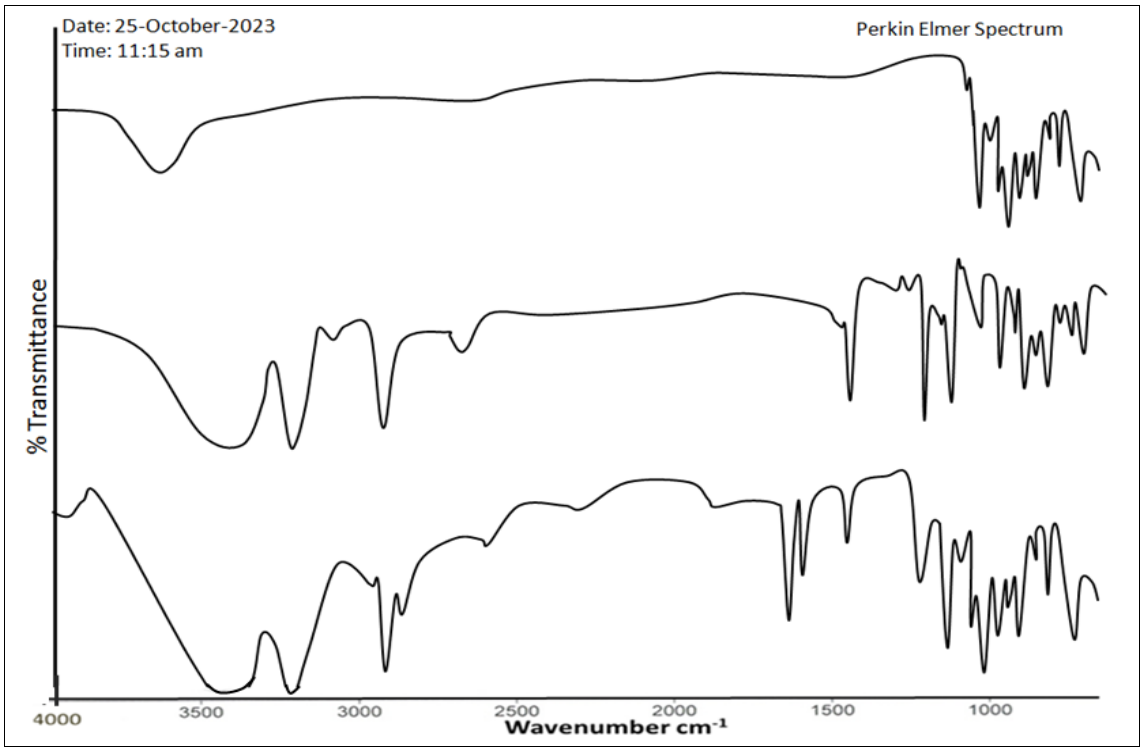

Fig 1: FT-IR (a) α-$K_8SiW_{11}O_{39}$ (b) LPOM-Sil (c) LPOM-Sil-HN

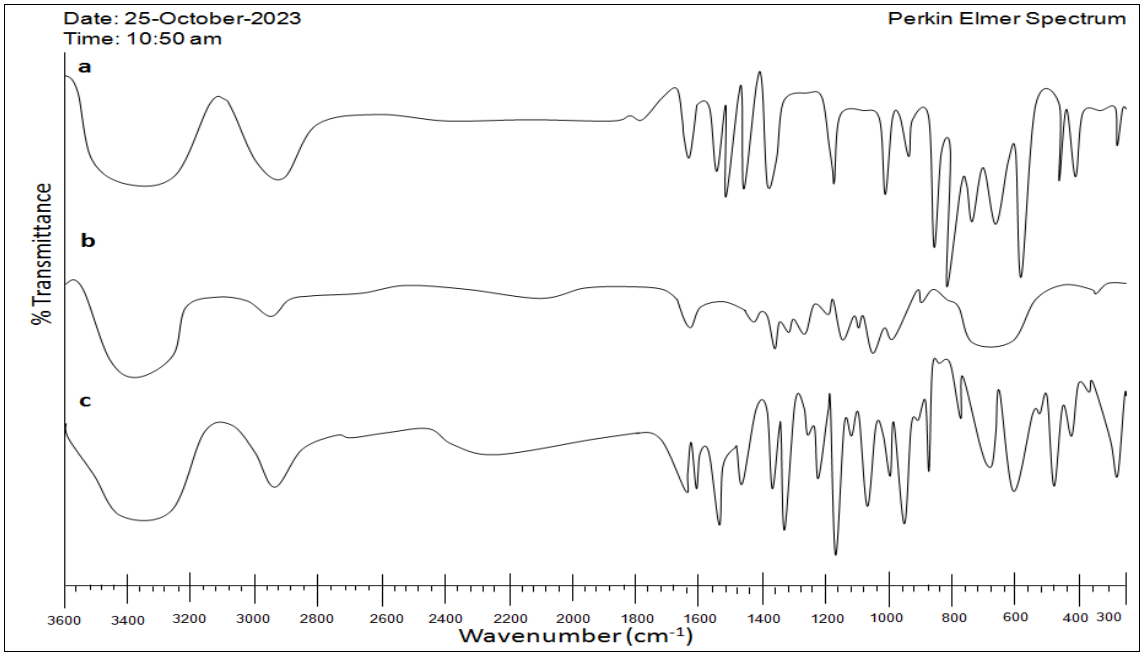

Fig 2: (a) LPOM-Sil-HN-Fe (b) CS (c) NHyd

3.2 EDX study

The stoichiometric ratio of the W atom from LPOM and the Fe atom present in NH is 11 atoms of W for every 1 atom of Fe, as further confirmed by the EDX study of the nanohybrid. This analysis also demonstrates the presence of all expected elements, such as C, N, and O in predictable ratios (Fig. 3).

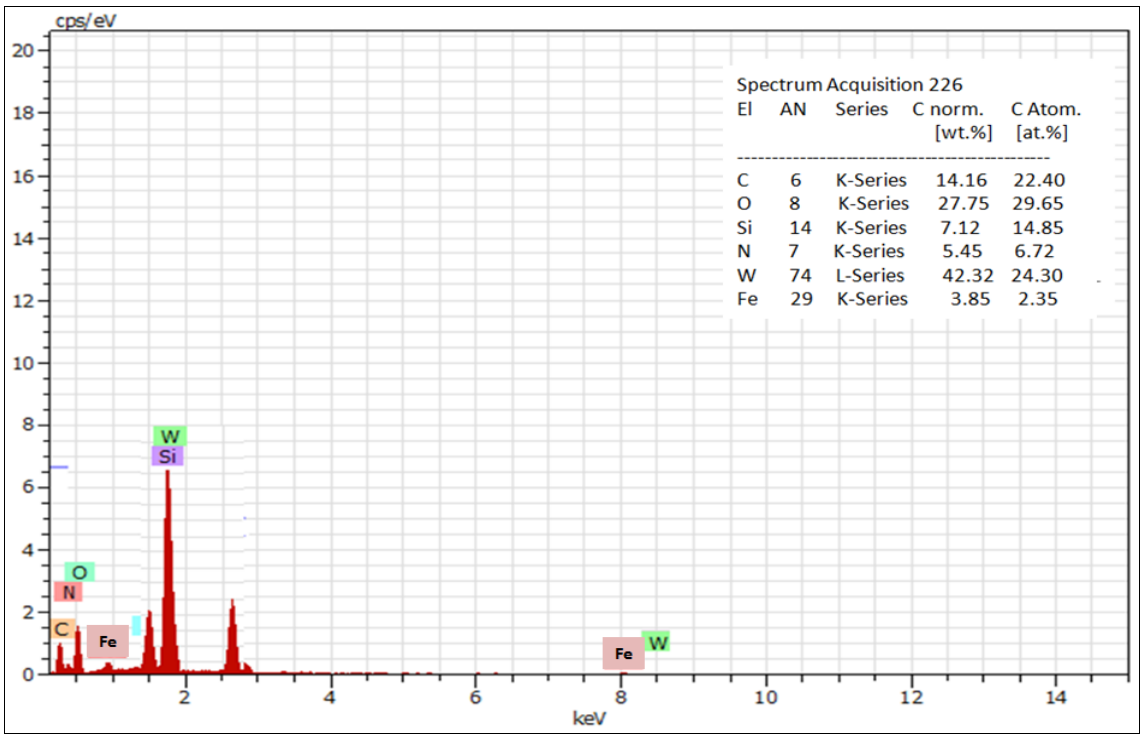

Fig 3: EDX of NHybd

3.3 UV-Vis-Spectroscopy

The absorption band in the 200–450 nm region of the UV–Vis spectrum of LPOM (α-$K_8SiW_{11}O_{39}$) in DMSO (Fig. 4a) has peaks at 209 and 265, which has been linked to the charge transfer transmission from O^{2-} to W^{6+} in Keggin type lacunary structure at W=O and W-O-W. Figure 4b displays the UV-Vis spectra of LPOM-Sil-NH-Fe. It indicates that the coordination geometry of the Fe(III) ion may be tetrahedral, with absorbance of the Fe(III) ion at 475 nm and 535 nm. The presence of two absorption peaks that were present in UV-Vis spectra of (α-$K_8SiW_{11}O_{39}$) with small shift in LPOM-Silane-2H1N-Fe indicate that alkylsilane was covalently linked to (α-$K_8SiW_{11}O_{39}$).

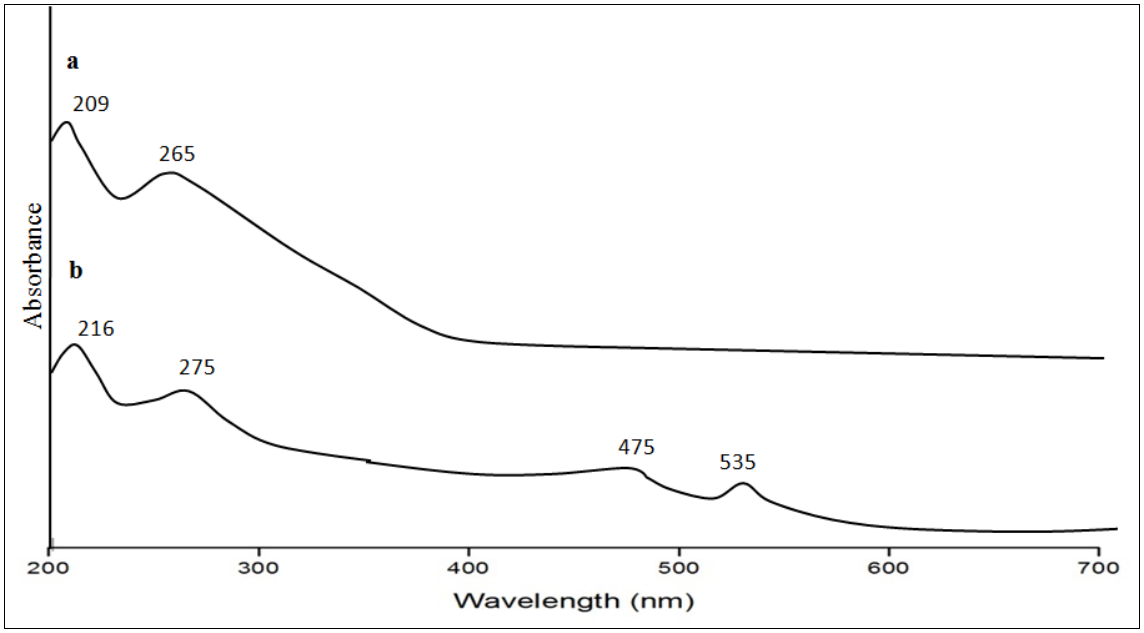

Fig 4(a): UV-Vis spectrum of LPOM (b) LPOM-Sil-NH-Fe

First, LPOM-Sil-NH-Fe UV-Vis spectra at a known concentration were captured (Fig. 5a). Then, while maintaining the same concentration of LPOM-Sil-NH-Fe during NH synthesis; four readings of the UV-Vis spectrum were obtained. The first supernatant reading was obtained immediately after the sonication was stopped (Fig. 5b), and the second supernatant reading was obtained after the colloidal suspension of LPOM-Sil-NH-Fe and CS had been continuously stirred for two hours (Fig. 5c). Following ten hours of nonstop stirring, the third reading (Fig. 5d) and fourth reading (Fig. 5e) of the supernatant were obtained. The typical LPOM-Sil-NH-Fe absorption peak is present in the first reading, but it is diminished in the second reading, indicating that LPOM-Sil-NH-Fe is trapped in CS. The characteristic peaks of LPOM-Sil-NH-Fe finally vanished in the third and fourth reading of UV-Vis spectra. This clearly indicates that LPOM-Sil-NH-Fe was successfully encapsulated into CS after centrifugation [17].

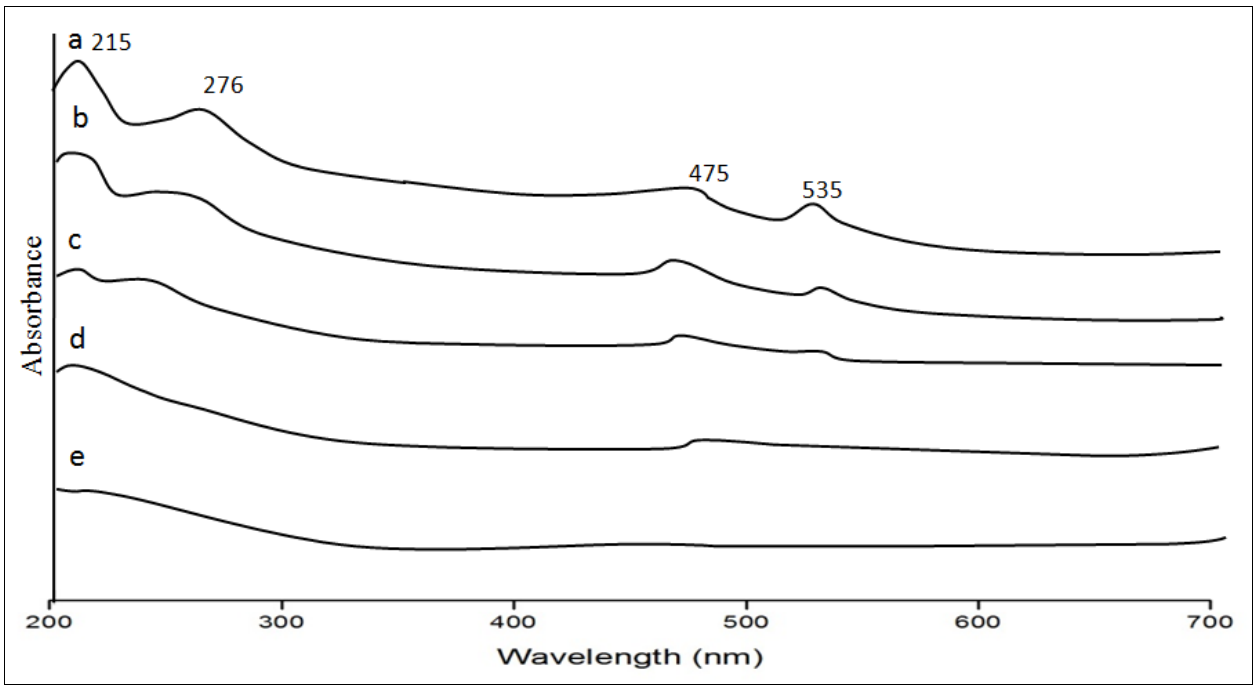

Fig 5: UV Vis Spectra of (a) LPOM-Sil-NH-Fe (b) First Reading was taken just after sonication of NHybd was stopped (c) Second reading after two hours of continuous stirring of colloidal suspension of NHybd (d) Third Reading after ten hours of continuous stirring of colloidal suspension of NHybd (e) Fourth Reading was taken after centrifugation of NHybd

3.4 Antibacterial Activity

Two bacterial strains, *B. subtilis (gram +ve)* and *E. Coli (gram –ve)*, were used to test the antibacterial qualities of LPOM-Sil-NH-Fe and NHybd. The results of these tests are tabulated in Figure 6. Because Fe ions are present, LPOM-Sil-NH-Fe exhibits possible antibacterial activity against both bacterial strains. Figure 6 makes it clear that, when compared to bare LPOM-Sil-NH-Fe, NHybd exhibits potential antimicrobial activity against both gram (+ve) and gram (-ve) bacteria. The positively charged amino groups in

chitosan may be interacting with the negatively charged phosphorous and sulfur compounds found in bacterial proteins and nucleic acid to cause structural alterations and deformation of the cell wall and membrane, which in turn results in cell death [18]. Enhanced antibacterial activity of the NHybd may also be attributed to its small size which can easily diffuse through membrane, hence affecting functioning of physiological activity of bacteria.

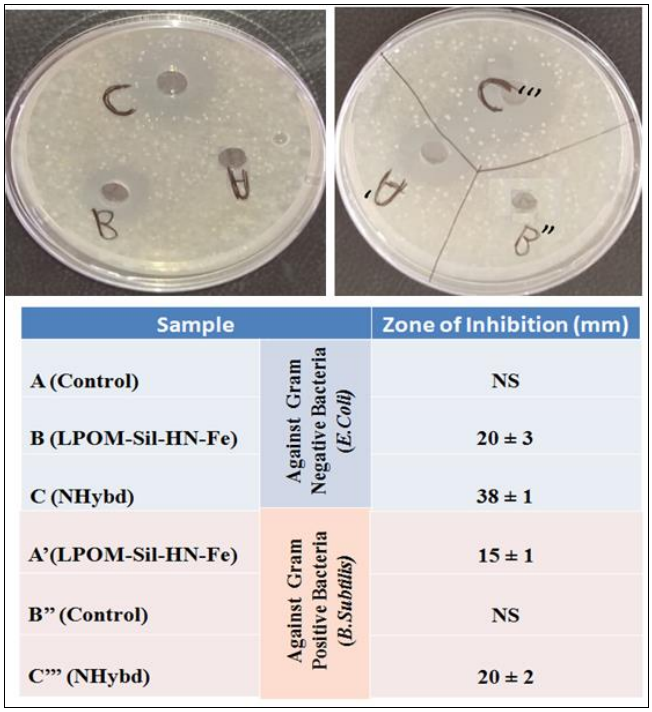

Sample		Zone of Inhibition (mm)
A (Control)	Against Gram Negative Bacteria (*E.Coli*)	NS
B (LPOM-Sil-HN-Fe)		20 ± 3
C (NHybd)		38 ± 1
A'(LPOM-Sil-HN-Fe)	Against Gram Positive Bacteria (*B.Subtilis*)	15 ± 1
B'' (Control)		NS
C''' (NHybd)		20 ± 2

Fig 6: Antibacterial assessment result against two different bacterial strains

Conclusion

In the present CS and POM based nanohybrid were formulated by simple and robust ionotropic gelation technique. The as prepared nanohybrid was characterized at each step by different characterization techniques. Antibacterial results also suggested their potential application for bacterial infections. Further, LPOM-Sil-HN-Fe can be studied by our research group for targeted treatment of tumor cells by drug delivery method.

Acknowledgement

SA is grateful to Hon'able Vice-chancellor Prof. R.K.P. Singh, Dr. Shakuntala Misra National Rehabilitation University Lucknow for University-Post Doctoral Fellowship (2209/1466 DSMNRU Research Cell 2020-21, dated 18 January 2022).

References

1. Dutta PK, Dutta J, Chattopadhyaya MC, Tripathi VS, Chitin, Chitosan. Novel biomaterials waiting for future developments, J. Polym. Mater. 2004;21:321-333.
2. Archana D, Dutta J, Dutta PK. Evaluation of chitosan nano dressing for wound healing: Characterization, *in vitro* and *in vivo* studies, International Journal of Biological Macromolecules. 2013;57:193-203.
3. Archana D, Singh BK, Dutta J, Dutta PK. Chitosan-PVP-nano silver oxide wound dressing: *In vitro* and *in vivo* evaluation, International Journal of Biological Macromolecules. 2015;73:49-57. (c) B. K. Singh, R. Sirohi, D. Archana, A. Jain P. K. Dutta, Porous Chitosan Scaffolds: A Systematic Study for Choice of Crosslinker and Growth Factor Incorporation, International Journal of Polymeric Materials and Polymeric Biometarials. 2014;64:242-252.
4. (a) Peng SF, Tseng MT, Ho YC, Wei MC, Liao ZX, Sung HW. Mechanisms of cellular uptake and intracellular trafficking with chitosan/DNA/poly (γ-glutamic acid) complexes as a gene delivery vector, Biomaterials. 2011;32:239-248. (b) Q. Zhao, X. Feng, S. Mei, Z. Jin, Carbon-nanotube-assisted high loading and controlled release of polyoxometalates in biodegradable multilayer thin films, Nanotechnology. 2009;20:105101.
5. Long DL, Burkholder E, Cronin L. Polyoxometalate clusters, nanostructures and materials: From self assembly to designer materials and devices, Chem. Soc. Rev. 2007;36:105-121; (b) T. Yamase, M. T. Pope, Polyoxometalate Chemistry for Nano-Composite Design, Kluwer, Dordrecht; c2002.
6. (a) Hasenknopf B. Polyoxometalates: Introduction To a Class Of Inorganic Compounds And Their Biomedical Applications, Front. Biosci. 2005;10:275-287; (b) J. T. Rhule, C. L. Hill, D. A. Judd, R. F. Schinazi, Polyoxometalates in Medicine, Chem. Rev. 1998;98: 327-357; (c) S. Arun, P. Bhartiya, A. Naz, S. Rai, S.S. Narvi, P.K. Dutta, Fabrication and Characterization of Polyoxometalate based Nano-hybrids: Evaluation of their role in Biological Activity, Journal of Polymer Materials, 35 (4) (2018) 473-482; (d) M. Witvrouw, H. Weigold, C. Pannecouque, D. Schols, E. De Clercq, G. Holan, Potent Anti-HIV (Type 1 and Type 2) Activity of Polyoxometalates: Structure−Activity Relationship and Mechanism of Action, J. Med. Chem., 43 (2000) 778 –783; (e) S. Shigeta, S. Mori, T. Yamase, N. Yamamoto, Anti-RNA virus activity of polyoxometalates, Biomed. Pharmacother. 2006;60:211-219.
7. Arun S, Singh VK, Naz A, Dutta PK. A comparative catalytic study using different metal ions by incorporating functionalized metallosalen into the lacunary position of Keggin polyoxometalate, Journal of the Indian Chemical Society. 2021;98:100118.
8. Zhang L, Chan JM, Gu FX, Rhee JW, Wang AZ, Radovic-Moreno AF, *et al*. Farokhzad, Self-Assembled Lipid−Polymer Hybrid Nanoparticles: A Robust Drug Delivery Platform, ACS nano. 2008;2:1696-1702.
9. Whitehead KA, Langer R, Anderson DG. Knocking down barriers: advances in siRNA delivery, Nature reviews Drug discovery. 2009;8:129-138.
10. Zhai F, Li D, Zhang C, Wang X, Li R. Synthesis and characterization of polyoxometalates loaded starch nanocomplex and its antitumoral activity, European Journal of Medicinal Chemistry. 2008;43:1911-1917.
11. (a) Bonchio M, Carraro M, Scorrano G, Fontananova E, Drioli E. Heterogeneous photooxidation of alcohols in water by photocatalytic membranes incorporating decatungstate, Adv. Synth. Catal. 2003;345:1119-1126. (b) G. Geisberger, S. Paulus, M. Carraro, M. Bonchio, G.R. Patzke, Synthesis, characterisation and cytotoxicity of polyoxometalate/carboxymethyl chitosan nanocomposites, Chem. Eur. J. 2011;17:4619-4625.
12. Teze A, Herve G, J Inor. Nucl. Chem. 1977;39:999.

13. Bar-Nahum I, Cohen H, Neumann R. Organometallic-Polyoxometalate Hybrid Compounds: Metallosalen Compounds Modified by Keggin Type Polyoxometalates Inorg. Chem. 2003;42:3677-3684.
14. Arun S. Fabrication of metallosalen compounds covalently linked to a Keggin type Polyoxometalate:Their characterization and catalytic study, Advances in Chemical and Applied Sciences, ISBN: 978-81-9350520-5. 2018;1:133.
15. (a) Menon D, Thomas RT, Narayanan S, Maya S, Jayakumar R, Hussain F, *et al*. A novel chitosan/polyoxometalate nano-complex for anti-cancer applications, Carbohydrate Polymers. 2011;84:887-893. (b) P. Bhartiya, R. Chawla, and P.K. Dutta, pH-Responsive Charge-Convertible N-Succinyl Chitosan-Quercetin Coordination Polymer Nanoparticles for Effective NIR Photothermal Cancer Therapy, Macromol. Chem. Phys; c2022, 2200140.
16. Bhartiya P, Chawla R, Dutta PK. Folate receptor targeted chitosan and polydopamine coated mesoporous silica nanoparticles for photothermal therapy and drug delivery, Journal of Macromolecular Science, Part A. 2022;59(12):810-817.
17. Helios K, Wysokinski R, Pietraszko A, Michalska D. Vibrational spectra and reinvestigation of the crystal structure of a polymeric copper(II)–orotate complex, $[Cu(\mu\text{-}HOr)(H_2O)_2]n$: The performance of new DFT methods, M06 and M05-2X, in theoretical studies, Vibrational Spectroscopy. 2011;55:207-215.
18. Naz A, Arun S, Narvi SS, Alam MS, Singh A, Bhartiya P, *et al*. Cu(II)-carboxymethyl chitosan-silane schiff base complex grafted onnano silica: Structural evolution, antibacterial performance and dyedegradation ability, International Journal of biological macromolecules. 2018;110:215-226.
19. Arun S, Singh Y, Naz A, Bhartiya P, Srivastava K, Narvi SS, *et al*. Chitosan Nano-composite containing Undecatungstosilicate via Cobalt Substitution: Characterization and Evaluation of their Biological Activity, J Polym. Mater. 2018;35(3):305-316.